

The Many Facets of Superfluidity in Dilute Fermi Systems

collaborators: Yongle Yu, P.F. Bedaque. A. C. Fonseca

Transparencies will be available shortly at
<http://www.phys.washington.edu/~bulgac>

One of my favorite times in the academic year occurs in early spring when I give my class of extremely bright graduate students, who have mastered quantum mechanics but are otherwise unsuspecting and innocent, a take-home exam in which they are asked to deduce superfluidity from first principles. There is no doubt a special place in hell being reserved for me at this very moment for this mean trick, for the task is impossible. Superfluidity, like the fractional quantum Hall effect, is an emergent phenomenon – a low-energy collective effect of huge numbers of particles that cannot be deduced from the microscopic equations of motion in a rigorous way and that disappears completely when the system is taken apart^{A)}. There are prototypes for superfluids, of course, and students who memorize them have taken the first step down the long road to understanding the phenomenon, but these are all approximate and in the end not deductive at all, but fits to experiment. The students feel betrayed and hurt by this experience because they have been trained to think in reductionist terms and thus to believe that everything not amenable to such thinking is unimportant. But nature is much more heartless than I am, and those students who stay in physics long enough to seriously confront the experimental record eventually come to understand that the reductionist idea is wrong a great deal of the time, and perhaps always.

Robert B. Laughlin, Nobel Lecture, December 8, 1998

Superconductivity and superfluidity in Fermi systems

- ✓ Dilute atomic Fermi gases $T_c > 10^{-12}$ eV
- Liquid ^3He $T_c > 10^{-7}$ eV
- Metals, composite materials $T_c > 10^{-3} - 10^{-2}$ eV
- Nuclei, neutron stars $T_c > 10^5 - 10^6$ eV
- QCD color superconductivity $T_c > 10^7 - 10^8$ eV

units (1 eV > 10⁴ K)

Memorable years in the history of superfluidity and superconductivity of Fermi systems

- 1913 Kamerlingh Onnes
- 1972 Bardeen, Cooper and Schrieffer
- 1973 Esaki, Giaever and Josephson
- 1987 Bednorz and Muller
- 1996 Lee, Osheroff and Richardson
- 2003 Abrikosov, Ginzburg and Leggett



Alexei A.
Abrikosov



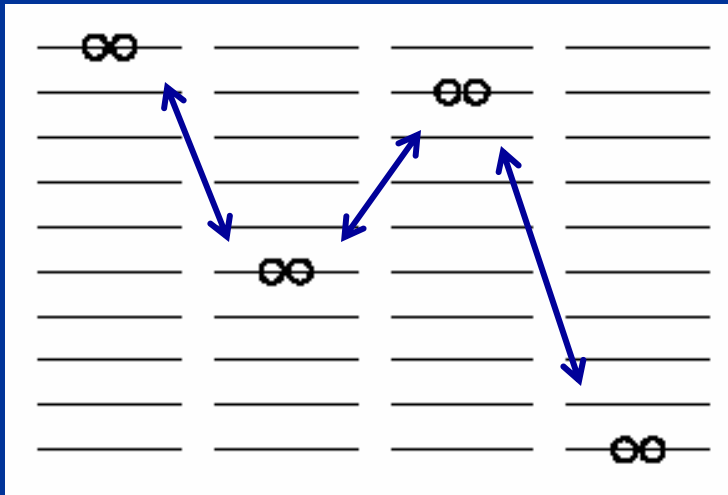
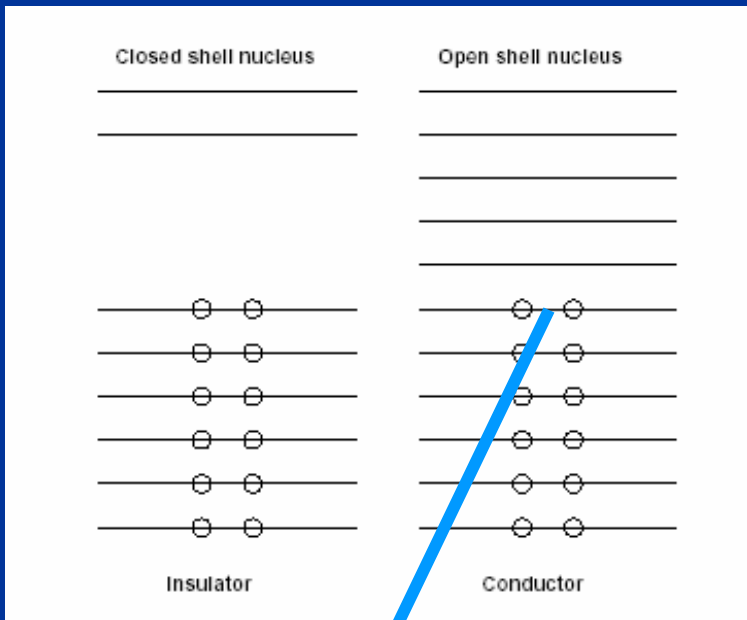
Vitaly L.
Ginzburg



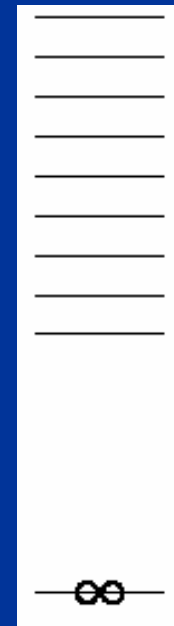
Anthony J.
Leggett

How pairing emerges?

Cooper's argument (1956)



Cooper pair



Gap 2D



In dilute Fermi systems only very few characteristics are relevant.

- These systems are typically very cold

$$T \ll T_F = \frac{\varepsilon_F}{k_B}, \quad \varepsilon_F = \frac{p_F^2}{2m}$$

- A dilute Fermi system is degenerate and the fastest particle has a momentum of the order of the Fermi momentum

$$p_F = (6\pi^2 n_{\uparrow})^{1/3} \hbar = (6\pi^2 n_{\downarrow})^{1/3} \hbar$$
$$n_{\uparrow} = n_{\downarrow} = \frac{n}{2}$$

- The wave functions are basically constant over the interaction volume of two particles and thus they cannot “see” any details, except the scattering length typically.

What is the scattering length?

$$k \cotan \delta_0(k) = -\frac{1}{a} + \frac{1}{2}r_0k^2 + \dots$$

$\left\{ \begin{array}{l} a > 0 \quad \text{a bound state exists} \end{array} \right.$

$\left\{ \begin{array}{l} a < 0 \quad \text{there is no bound state} \end{array} \right.$

$$\psi(\vec{r}) = \exp(i\vec{k} \cdot \vec{r}) + \frac{f}{r} \exp(ikr) \underset{kr \rightarrow 0}{\approx} 1 - \frac{a}{r} + O(kr)$$

 In the region outside the potential well

At very low energies the interaction of two particles can be approximated by the “potential”

$$U(\vec{r}) = \frac{4\pi\hbar^2 a}{m} \delta(\vec{r}) = \begin{cases} > 0 \text{ (repulsive)} & \text{if } a > 0 \\ < 0 \text{ (attractive)} & \text{if } a < 0 \end{cases}$$

In dilute atomic systems experimenters can control nowadays almost anything:

- The number of atoms in the trap
- The density of atoms
- Mixtures of various atoms
- The temperature of the atomic cloud
- The strength of the atom-atom interaction

HISTORY

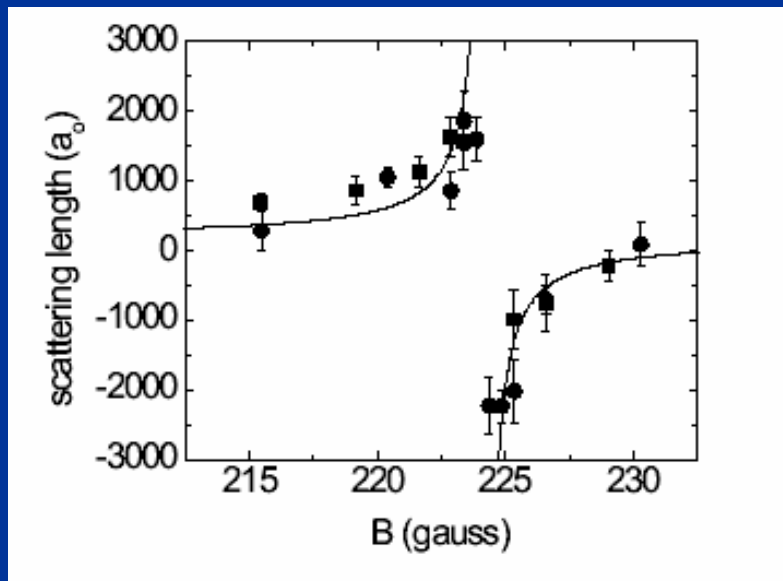
- ✓ 1995 BEC was observed.
- ✓ 2000 vortices in BEC were created
thus BEC confirmed un-ambiguously.
- ✓ In 1999 DeMarco and Jin created a degenerate atomic Fermi gas.
- ✓ 2002 O'Hara, Hammer, Gehm, Granada and Thomas observed expansion of a Fermi cloud compatible with the existence of a superfluid fermionic phase.
- ✓ 2003 Jin's, Grimm's, Ketterle's groups and others ultracold molecules, mBEC from Fermi gas
- ✓ 2004 Jin's group announces the observation of the resonance condensation of fermionic atomic pairs ?

Feshbach resonance

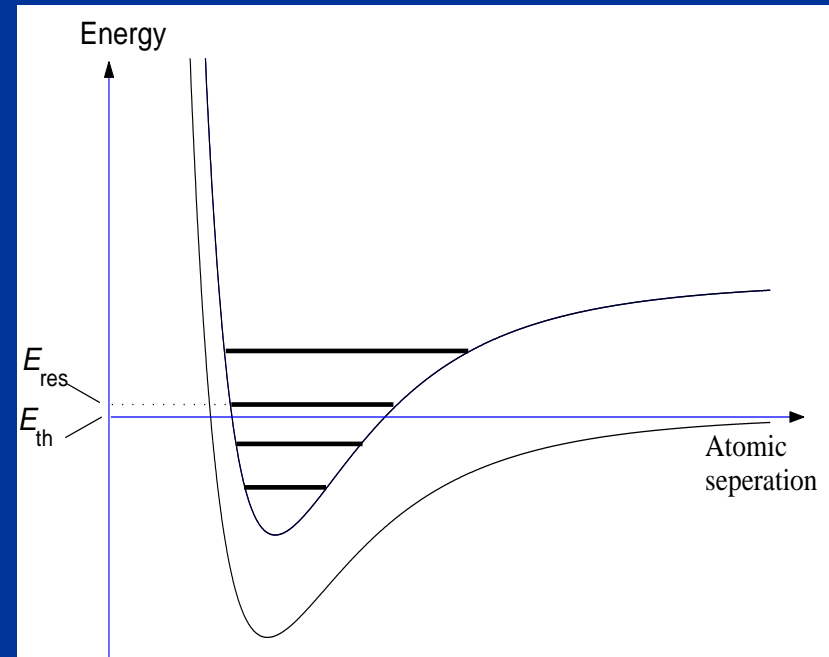
$$H = \frac{\vec{p}^2}{2\mu_r} + \sum_{i=1}^2 (V_i^{hf} + V_i^Z) + V_0(\vec{r})P_0 + V_1(\vec{r})P_1 + V^d$$

$$V^{hf} = \frac{a_{hf}}{\hbar^2} \vec{S}^e \cdot \vec{S}^n, \quad V^Z = (\gamma_e S_z^e - \gamma_n S_z^n) B$$

Tiesinga, Verhaar, Stoof
Phys. Rev. A 47, 4114 (1993)



Regal and Jin
Phys. Rev. Lett. 90, 230404 (2003)



BCS \rightarrow BEC crossover

Leggett (1980), Nozieres and Schmitt-Rink (1985), Randeria *et al.* (1993)

If $a < 0$ at $T=0$ a Fermi system is a BCS superfluid

$$\Delta \approx \left(\frac{2}{e}\right)^{7/3} \frac{\hbar^2 k_F^2}{2m} \exp\left(\frac{\pi}{2k_F a}\right), \quad \text{iff } k_F |a| \ll 1 \text{ and } \xi = \frac{1}{k_F} \frac{\varepsilon_F}{\Delta} \gg \frac{1}{k_F}$$

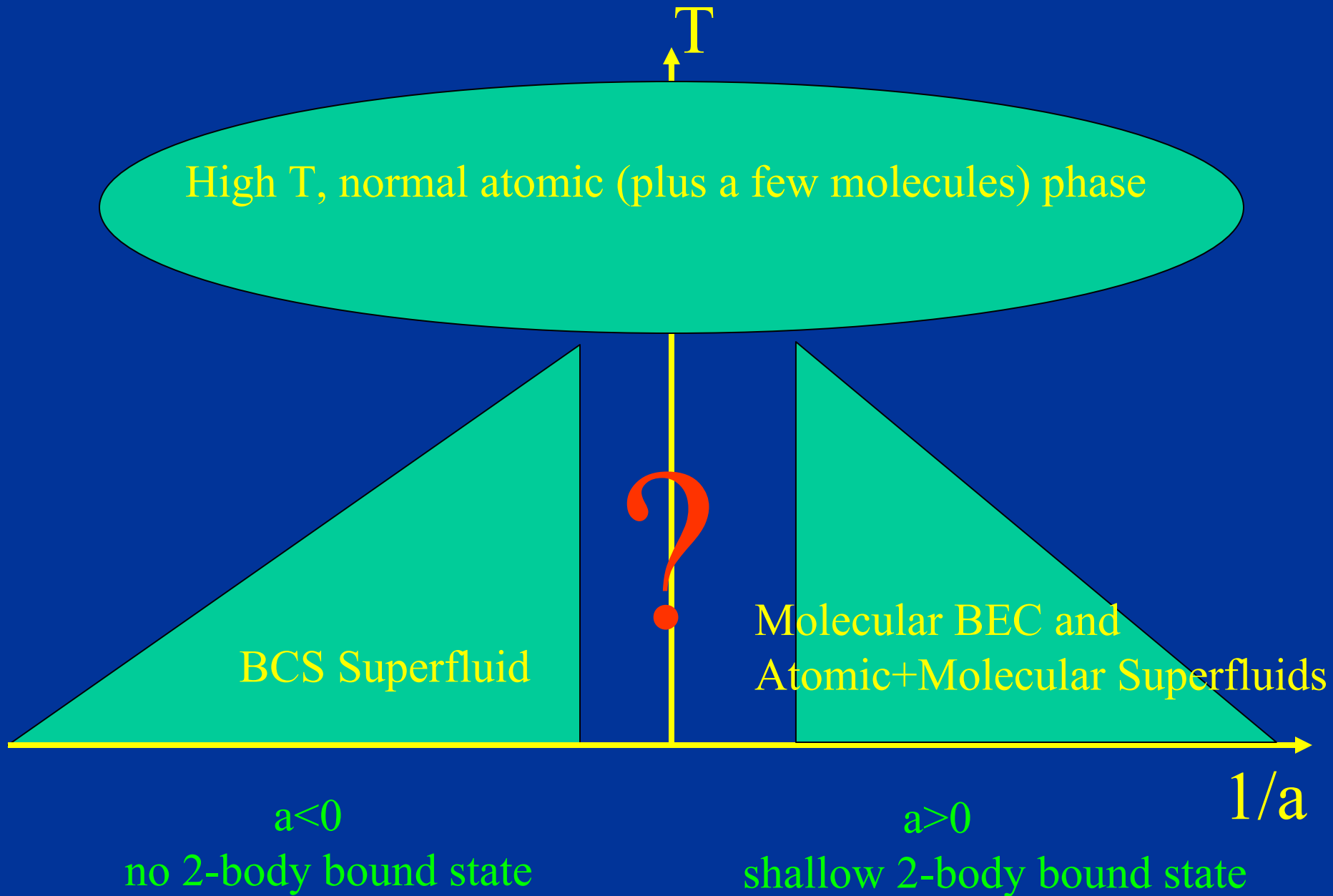
If $|a| = \infty$ and $n r_0^3 \hat{a} \ll 1$ a Fermi system is strongly coupled and its properties are universal. Carlson *et al.* PRL 91, 050401 (2003)

$$\frac{E_{\text{normal}}}{N} \approx 0.54 \frac{3}{5} \varepsilon_F, \quad \frac{E_{\text{superfluid}}}{N} \approx 0.44 \frac{3}{5} \varepsilon_F \quad \text{and } \xi = O(\lambda_F)$$

If $a > 0$ ($a \gg r_0$) and $n a^3 \hat{a} \ll 1$ the system is a dilute BEC of tightly bound dimers

$$\varepsilon_2 = -\frac{\hbar^2}{m a^2} \quad \text{and} \quad n_b a^3 \ll 1, \quad \text{where } n_b = \frac{n_f}{2} \quad \text{and} \quad a_{bb} = 0.60 a > 0$$

Expected phases of a two species dilute Fermi system



High T , normal atomic (plus a few molecules) phase

BCS Superfluid

Molecular BEC and
Atomic+Molecular Superfluids

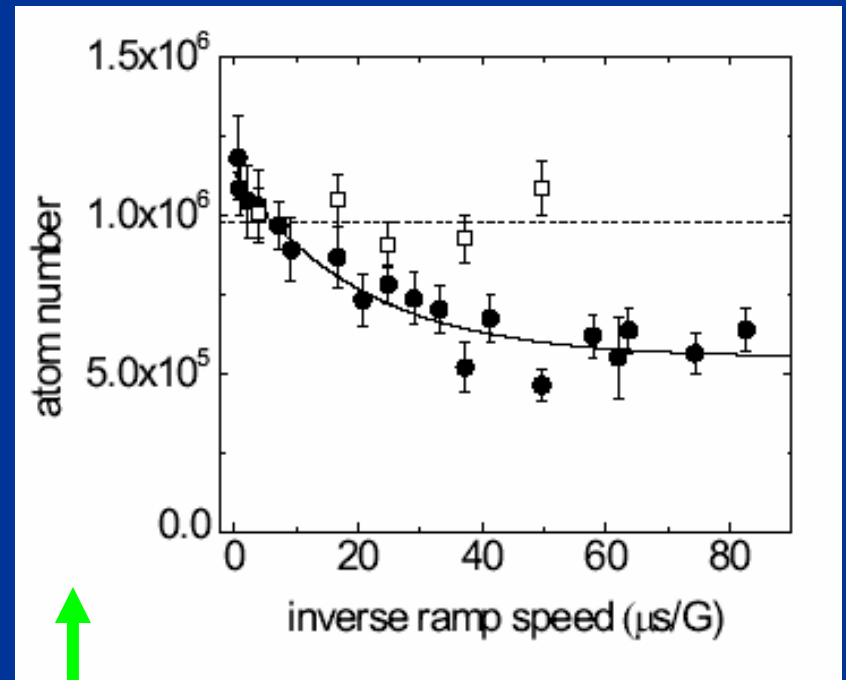
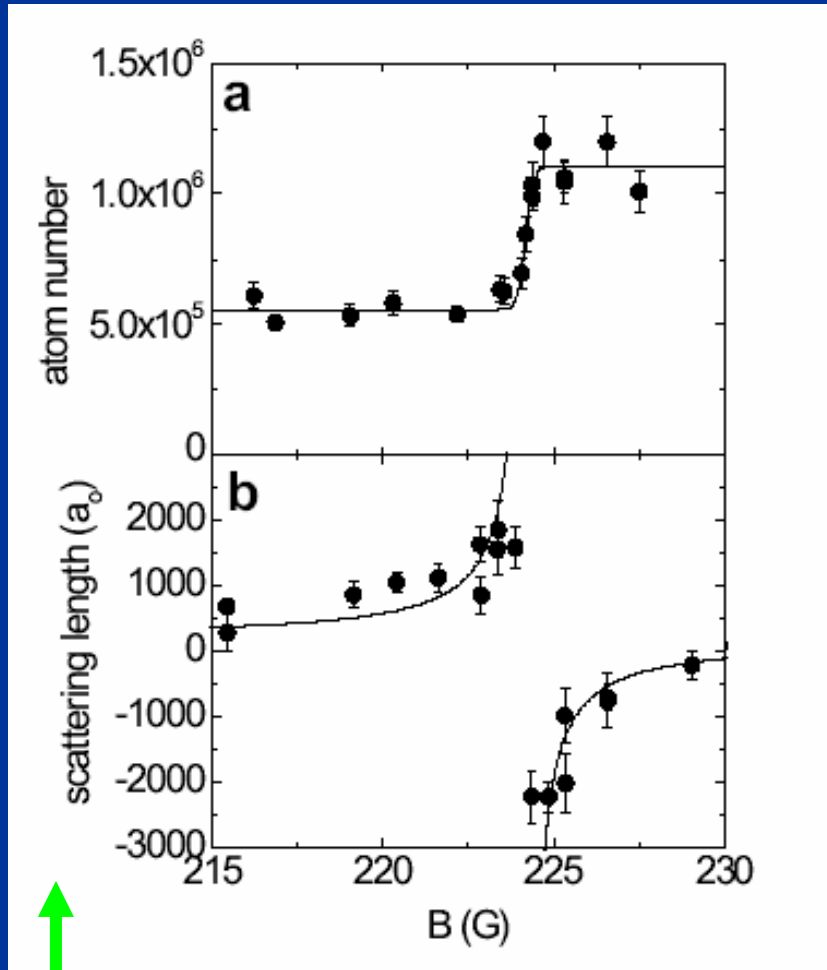
$a < 0$

no 2-body bound state

$a > 0$

shallow 2-body bound state

$1/a$



Number of atoms after ramping B from 228.25 G to 216.15 (black dots) and for ramping B down (at 40 ns/G) and up at various rates (squares).

- Loss of atoms $|9/2, -9/2\rangle$ and $|9/2, -5/2\rangle$ as a function of final B . The initial value of $B = 227.81$ G.
- Scattering length between hyperfine states $|9/2, -9/2\rangle$ and $|9/2, -5/2\rangle$ as a function of the magnetic field B .

Symmetric peak is near the atomic $|9/2, -5/2\rangle$ to $|9/2, -7/2\rangle$ transition. The total number of $|9/2, -5/2\rangle$ and $|9/2, -7/2\rangle$ atoms is constant.

Asymmetric peak corresponds to dissociation of molecules into free $|9/2, -5/2\rangle$ and $|9/2, -7/2\rangle$ atoms. The total number of $|9/2, -5/2\rangle$ and $|9/2, -7/2\rangle$ atoms increases.

$$h\nu_{rf} = h\nu_{atom} - E_{binding} - \Delta E$$

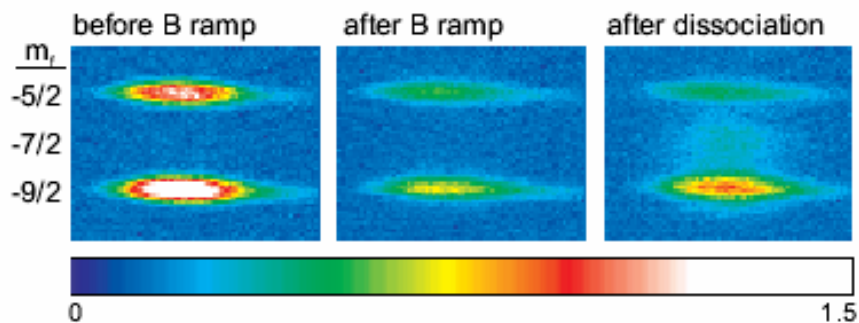
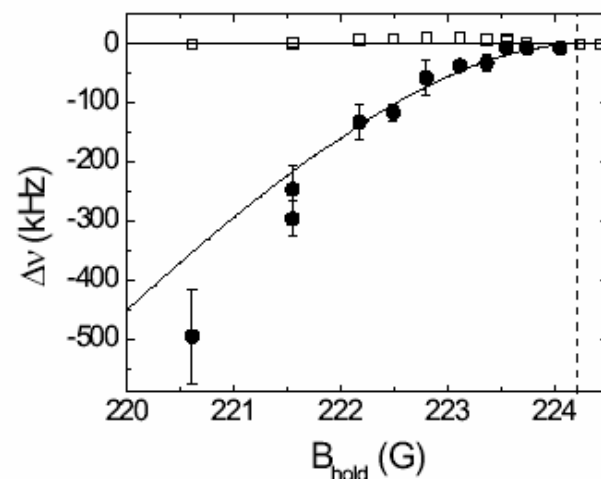
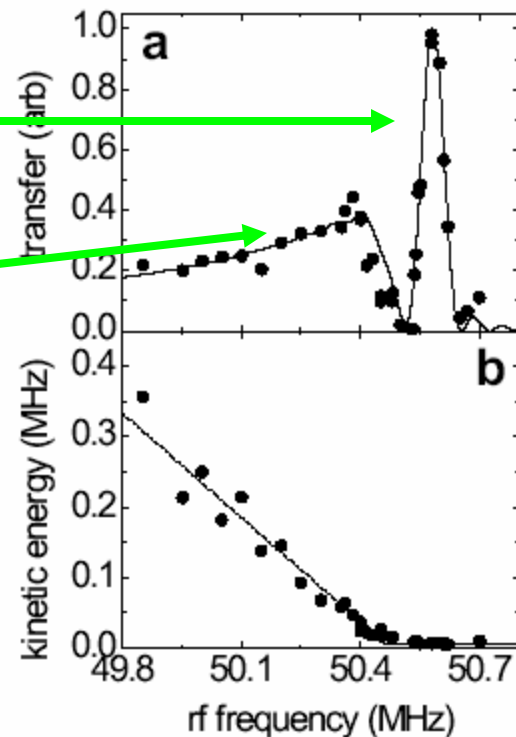


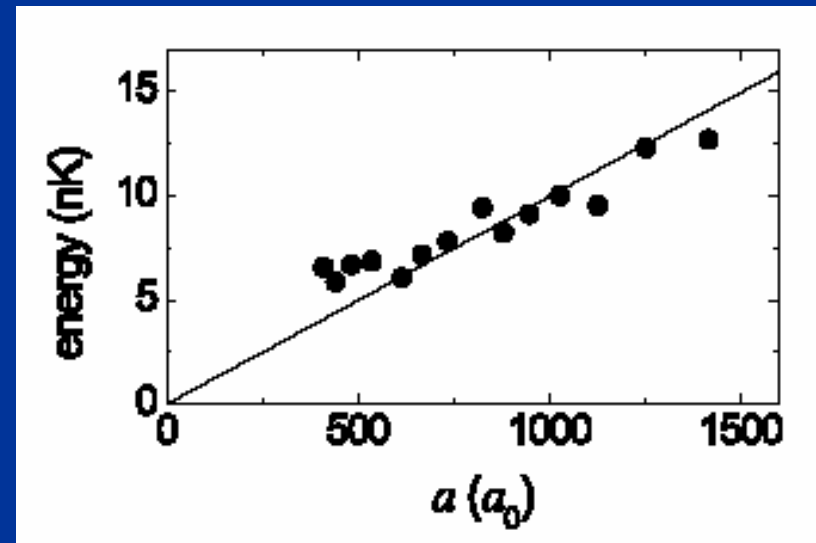
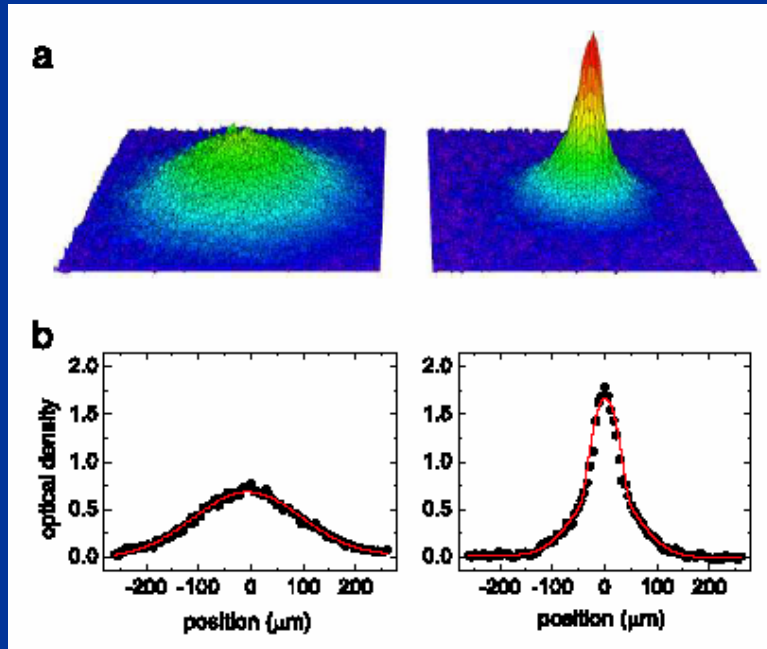
FIG. 4: Absorption images of the quantum gas using a Stern-Gerlach technique. We start with ultracold fermionic atoms in the $|9/2, -5/2\rangle$ and $|9/2, -9/2\rangle$ states of ^{40}K . A magnetic field ramp through the Feshbach resonance causes 50% atom loss, due to adiabatic conversion of atoms to diatomic molecules. To directly detect these bosonic molecules we apply an rf photodissociation pulse; the dissociated molecules then appear in the $|9/2, -7/2\rangle$ and $|9/2, -9/2\rangle$ atom states. The shaded bar indicates the optical depth.



Dimer/molecule binding energy

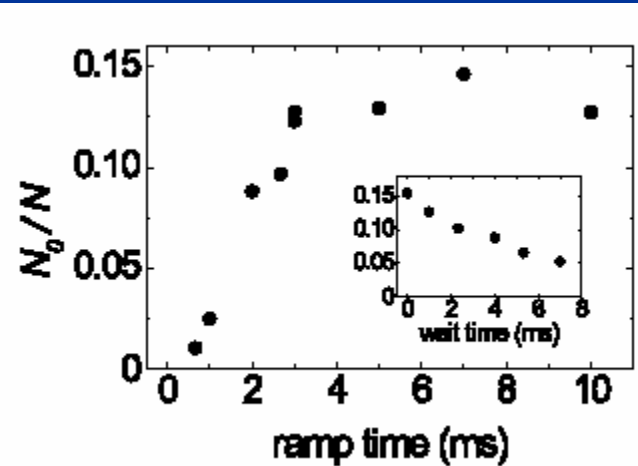
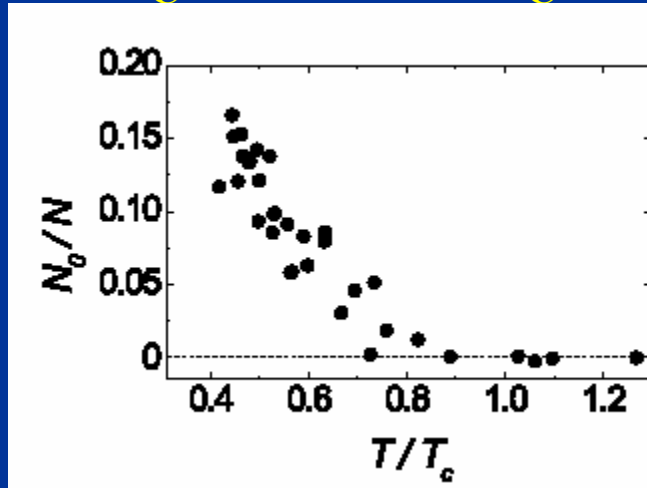
Molecular BEC in a cloud of ^{40}K atoms (fermions)

Greiner, Regal and Jin, Nature 426, 537 (2003)

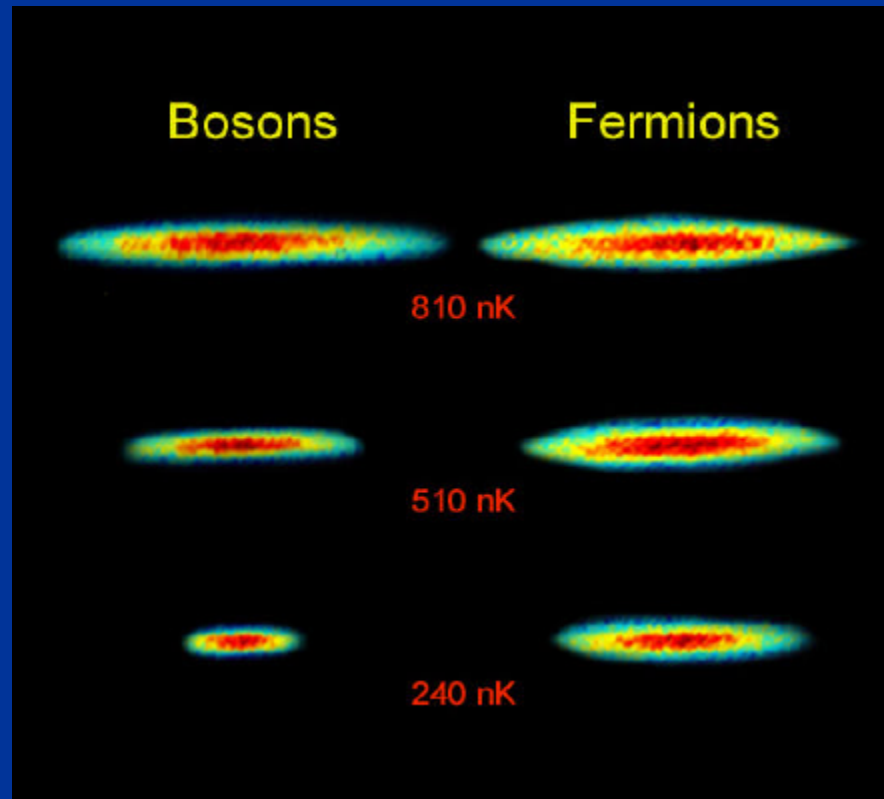


$T > T_c$

$T < T_c$



Size of the atomic cloud as a function of temperature around the critical temperature



Grimm's group

cond-mat/04010109

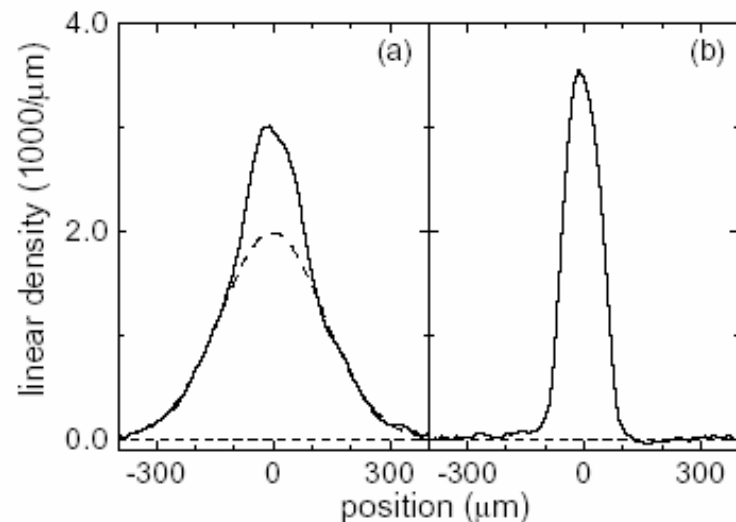


FIG. 1: Axial density profiles of a partially condensed (a) and fully condensed (b) molecular cloud. The profiles are derived from in situ images taken at a magnetic field of $B = 676\text{G}$ after evaporation at the production field of 764G . (a) When the evaporation ramp is stopped with 4×10^5 molecules at a final laser power of 28 mW , a characteristic bimodal distribution is observed with a condensate fraction of $\sim 20\%$. The dashed curve shows the thermal fraction of $\sim 80\%$. (b) At a final laser power of 3.8 mW , an essentially pure condensate of 2×10^5 molecules is obtained.

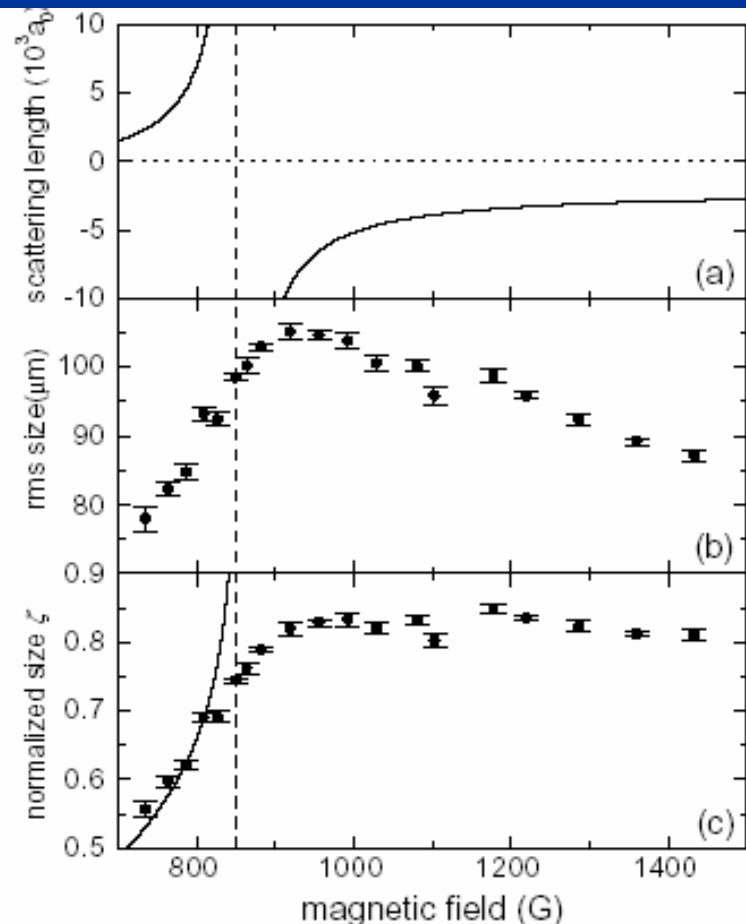


FIG. 3: Axial cloud size measurements across the Feshbach resonance. In (a) the atomic scattering length a is shown according to [16]; the resonance at 850 G is marked by the vertical dashed line. The data in (b) display the measured rms cloud sizes. In (c), the same data are replotted after normalization to a non-interacting Fermi gas. The solid line shows the expectation from BEC mean-field theory with $a_m = 0.6 a$. In (b) and (c), the error bars show the statistical error of the size measurements from typically five individual images.

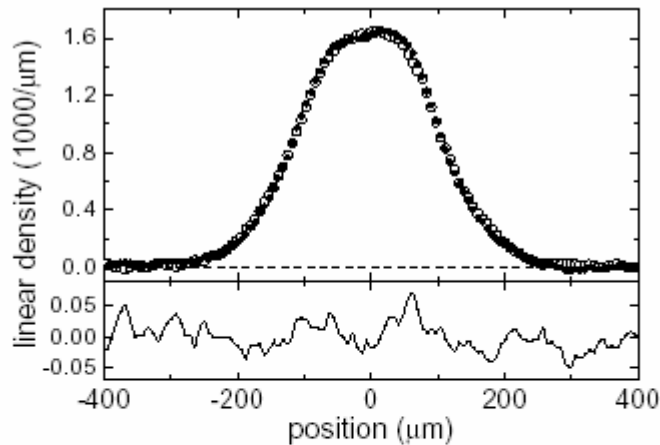


FIG. 2: Axial profile of a molecular BEC at 764 G (●) after its conversion into a Fermi gas at 1176 G and subsequent back-conversion. Two 1-s magnetic field ramps are applied in this reversible process. For reference we show the corresponding profile observed without the magnetic field ramp (○). The density profiles are obtained by averaging over 50 images. The difference shown in the lower graph is consistent with the drifts of a residual interference pattern in the images [23].

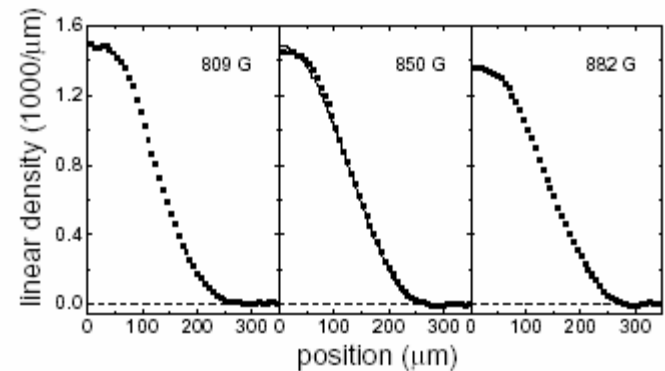


FIG. 4: Observed axial density profiles near the Feshbach resonance, averaged over 50 images and symmetrized to reduce imaging imperfections. The rms cloud sizes are $93 \mu\text{m}$, $99 \mu\text{m}$, and $103 \mu\text{m}$ at $B = 809\text{G}$, 850G , and 882G , respectively. For comparison, the on-resonance data at 850 G are shown together with a fit by the expected profile $\propto (1 - z^2/z_{\text{TF}}^2)^{5/2}$. The small deviation near the top is due to a residual interference pattern in the images.

Grimm's group, cond-mat/04010109

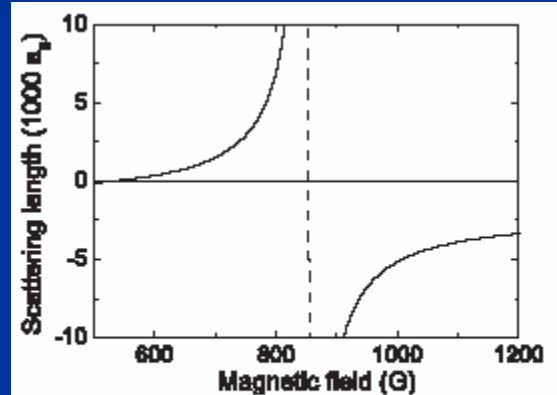


Fig. 1. Feshbach resonance at $\sim 850 \text{ G}$ in a mixture of the two lowest spin states of ${}^6\text{Li}$ (18). The s -wave scattering length a is plotted as a function of the magnetic field B .

Scientists Create New Form of Matter

REUTERS 

Wed Jan 28, 4:05 PM ET

 Add [Science - Reuters](#) to My Yahoo!

By Maggie Fox, Health and Science Correspondent

WASHINGTON (Reuters) - Scientists said on Wednesday they had created a new form of matter and predicted it could help lead to the next generation of superconductors for use in electricity generation, more efficient trains and countless other applications.

"What we've done is create this new exotic form of matter," Deborah Jin, a physicist at the National Institute of Standards and Technology's joint lab with the University of Colorado, who led the study, told a news conference.

Physical Review Letters

30 January 2004

Phys. Rev. Lett. **92**, 040403 (2004)

Observation of Resonance Condensation of Fermionic Atom Pairs

[C. A. Regal](#), [M. Greiner](#), and [D. S. Jin](#)

JILA, National Institute of Standards and Technology and University of Colorado, and Department of Physics, University of Colorado, Boulder, Colorado 80309-0440, USA

(Received 13 January 2004; published 28 January 2004)

We have observed condensation of fermionic atom pairs in the BCS-BEC crossover regime. A trapped gas of fermionic ^{40}K atoms is evaporatively cooled to quantum degeneracy and then a magnetic-field Feshbach resonance is used to control the atom-atom interactions. The location of this resonance is precisely determined from low-density measurements of molecule dissociation. In order to search for condensation on either side of the resonance, we introduce a technique that pairwise projects fermionic atoms onto molecules; this enables us to measure the momentum distribution of fermionic atom pairs. The transition to condensation of fermionic atom pairs is mapped out as a function of the initial atom gas temperature T compared to the Fermi temperature T_F for magnetic-field detunings on both the BCS and BEC sides of the resonance. ©2004 The American Physical Society

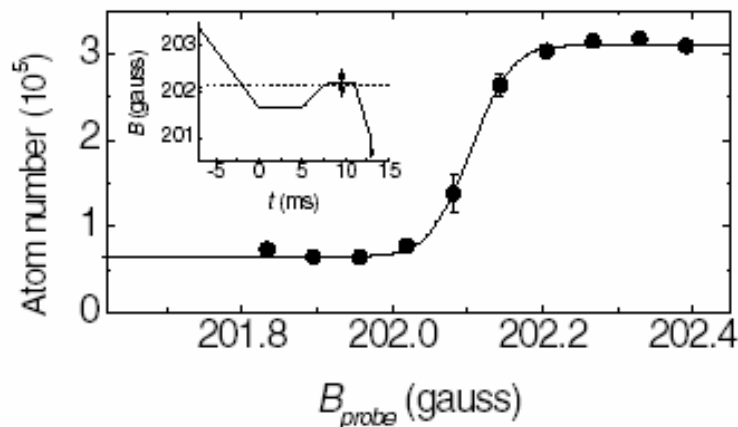


FIG. 1. Measurement of the Feshbach resonance position B_0 . Shown in the inset is a schematic of the magnetic field as a function of time t measured with respect to the optical trap turn off at $t = 0$. Molecules are first created by a slow magnetic-field sweep across the resonance (dotted line) and then dissociated if B_{probe} (indicated by the arrow in the inset) is beyond the magnetic field where the two-body physics supports a new bound state. The number of atoms, measured at $t = 17$ ms, is shown as a function of B_{probe} . The two error bars indicate the spread in repeated points at these values of B . A fit of the data to an error function reveals $B_0 = 202.10 \pm 0.07$ G, where the uncertainty is given conservatively by the 10%–90% width.

$$a(B) = a_{bg} \left(1 - \frac{w}{B - B_0} \right)$$

$$a_{bg} = 174a_0$$

$$w = 7.8 \pm 0.6 \text{ G}$$

$$B_0 = 202.10 \pm 0.07 \text{ G}$$

$a > 0$

$a < 0$

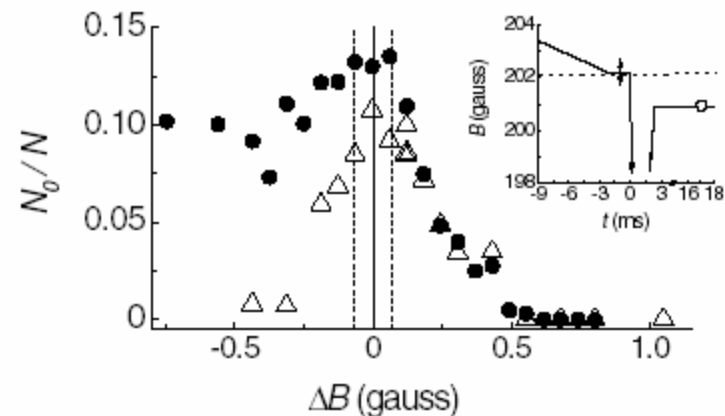


FIG. 2. Measured condensate fraction as a function of detuning from the Feshbach resonance $\Delta B = B_{\text{hold}} - B_0$. Data here were taken for $t_{\text{hold}} = 2$ ms (\bullet) and $t_{\text{hold}} = 30$ ms (\triangle) with an initial cloud at $T/T_F = 0.08$ and $T_F = 0.35 \mu\text{K}$. The area between the dashed lines around $\Delta B = 0$ reflects the uncertainty in the Feshbach resonance position based on the 10%–90% width of the feature in Fig. 1. Condensation of fermionic atom pairs is seen near and on either side of the Feshbach resonance. Comparison of the data taken with the different hold times indicates that the pair condensed state has a significantly longer lifetime near the Feshbach resonance and on the BCS ($\Delta B > 0$) side. The inset shows a schematic of a typical magnetic-field sweep used to measure the fermionic condensate fraction. The system is first prepared by a slow magnetic-field sweep towards the resonance (dotted line) to a variable position B_{hold} , indicated by the two-sided arrow. After a time t_{hold} the optical trap is turned off and the magnetic field is quickly lowered by ~ 10 G to project the atom gas onto a molecular gas. After free expansion, the molecules are imaged on the BEC side of the resonance (\circ).

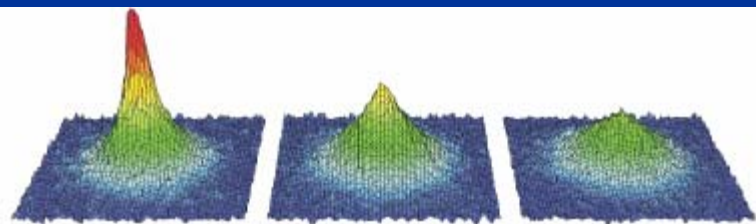
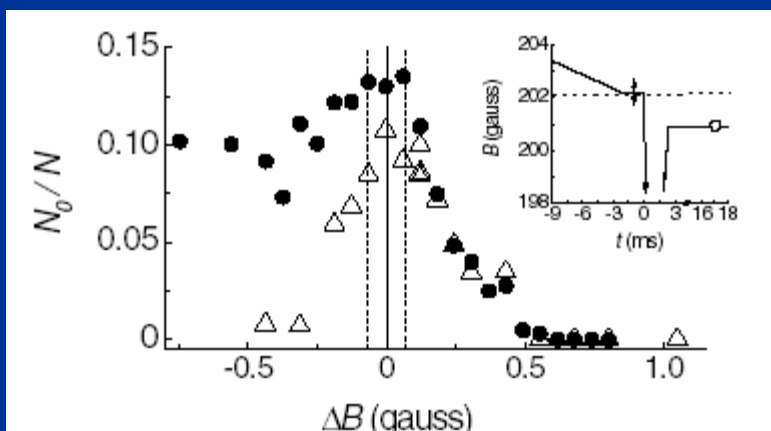


FIG. 3 (color online). Time of flight images showing the fermionic condensate. The images, taken after the projection of the fermionic system onto a molecular gas, are shown for $\Delta B = 0.12, 0.25,$ and 0.55 G (left to right) on the BCS side of the resonance. The original atom cloud starts at $T/T_F = 0.07$, and the resulting fitted condensate fractions are $N_0/N = 0.10, 0.05,$ and 0.01 (left to right). Each image corresponds to $N = 100\,000$ particles and is an average over 10 cycles of the experiment.

$a > 0$

$a < 0$



$$|k_F a| > 1$$

BEC side

BCS side

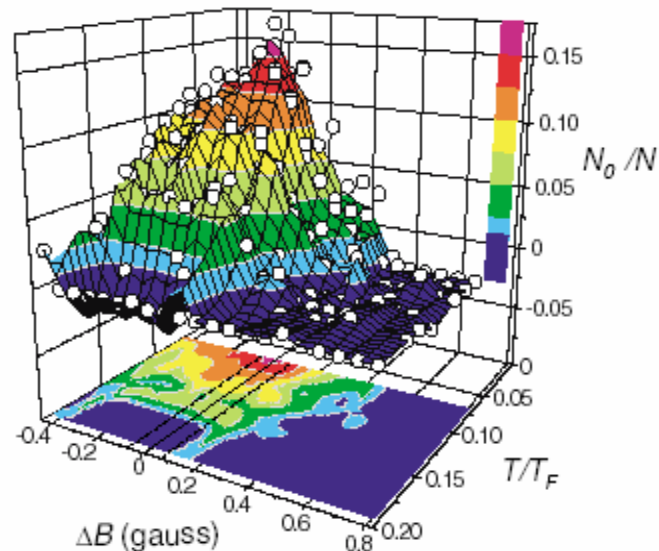


FIG. 4 (color online). Transition to condensation as a function of both ΔB and T/T_F . The data for this phase diagram were collected with the same procedure as shown in the inset in Fig. 2 with $t_{\text{hold}} \sim 2$ ms. The area between the dashed lines around $\Delta B = 0$ reflects the uncertainty in the Feshbach resonance location from the width of the feature in Fig. 1. The surface and contour plots are obtained using a Renka-Cline interpolation of approximately 200 distinct data points (\circ) [36]. One measure of when the gas becomes strongly interacting is the criterion $|k_F a| > 1$, where $\hbar k_F$ is the Fermi momentum [20,21,37,38]. For these data, $|\Delta B| < 0.6$ corresponds to $|k_F a| > 1$.

?

molecules. However, we find that there is a threshold curve of T/T_F versus detuning from the Feshbach resonance below which we observe a fraction of the molecules to have near zero momentum. We interpret this as reflecting a preexisting condensation of fermionic atom pairs.

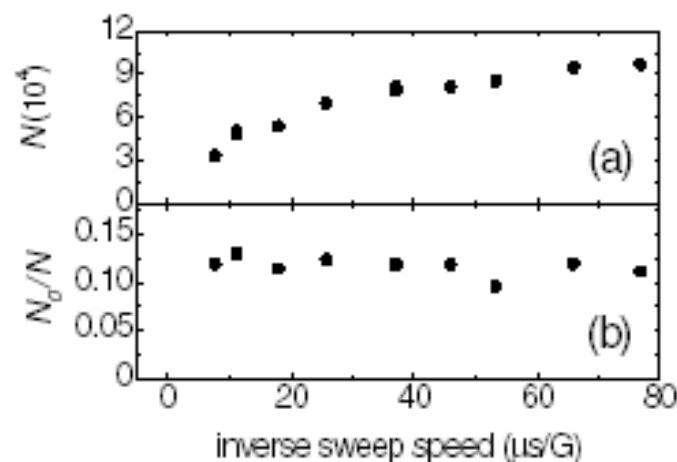


FIG. 5. Dependence of molecule number and condensate fraction on the speed of the fast magnetic-field sweep from the atomic gas onto the molecular gas. Here $\Delta B = 0.12$ and the initial T/T_F is 0.08. (a) Total number of molecules as a function of inverse sweep speed. For the fastest sweep speeds fewer molecules are created, consistent with studies in Ref. [11]. (b) Condensate fraction as a function of the inverse sweep speed. Even for the fastest sweeps and lowest molecule number, we observe an unchanged condensate fraction.

What did they see in this last experiment?

Did they put in evidence a BCS-like superfluid?

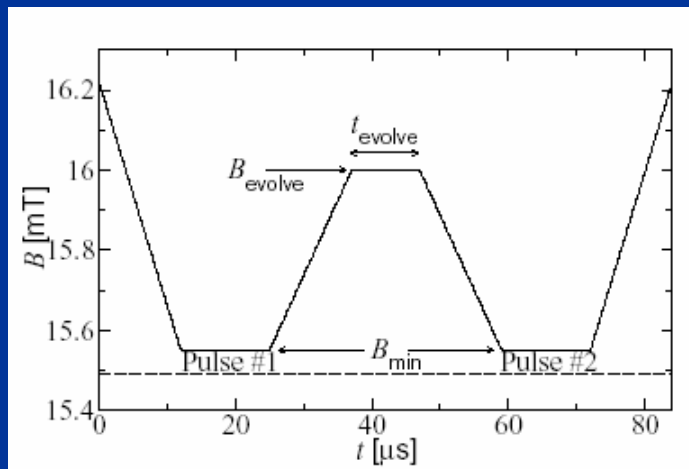
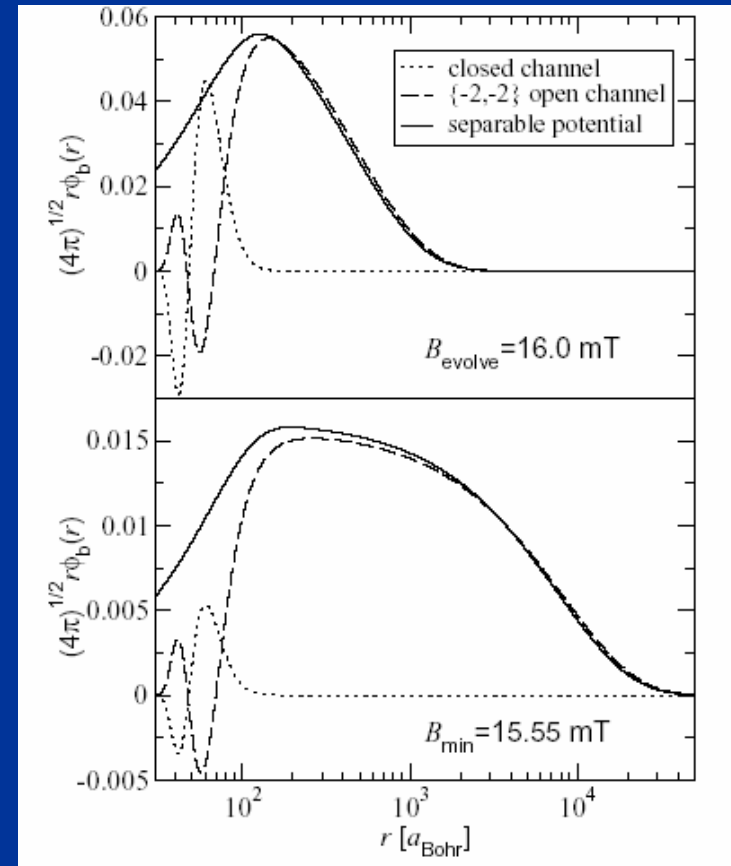
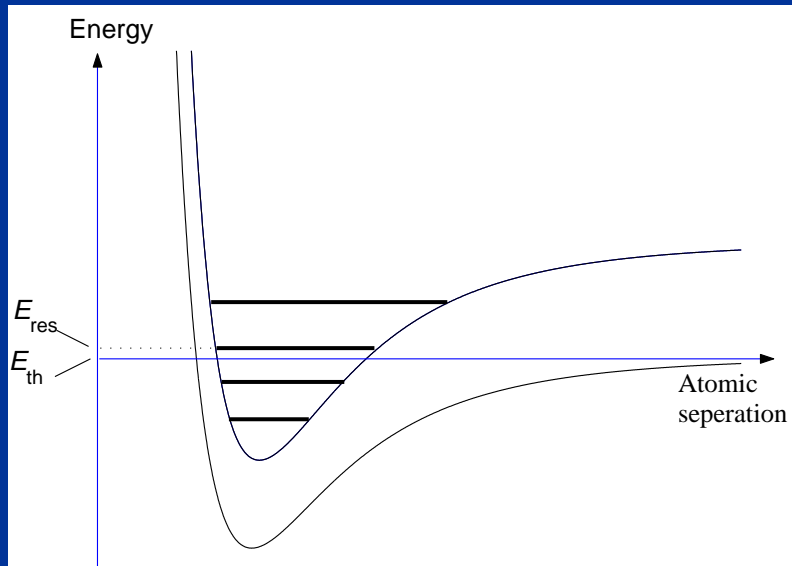
What was the order parameter?

Assuming that they've determined correctly

T_c for $|a| \rightarrow \infty$ one would get $T_c \approx 0.3\Delta$

NB T_c is unknown both theoretically and experimentally in the strong coupling limit.

Köhler, Gasenzer, Jullienne and Burnett
 PRL 91, 230401 (2003).



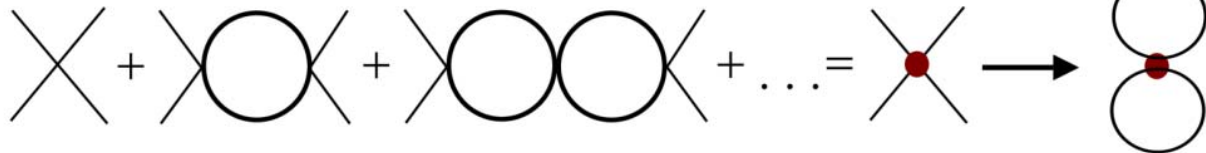
$$\frac{P(r > r_0)}{P(r < r_0)} \propto \frac{a}{r_0} \gg 1$$

NB The size of the “Feshbach molecule” (closed channel state) is largely B-independent and smaller than the interparticle separation.

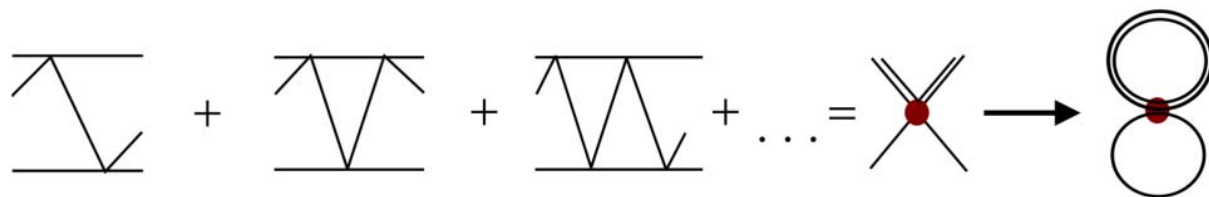
We need a well defined procedure for constructing an “effective” Hamiltonian for interacting atoms and dimers starting from the “fundamental” Hamiltonian describing bare interacting atoms.

$$H_{am} = \psi_a^+ \left(-\frac{\hbar^2 \nabla^2}{2m} \right) \psi_a + \psi_m^+ \left(-\frac{\hbar^2 \nabla^2}{4m} + \varepsilon_2 \right) \psi_m \\ + \frac{1}{2} \lambda_{aa} \psi_a^+ \psi_a^+ \psi_a \psi_a + \lambda_{am} \psi_a^+ \psi_m^+ \psi_m \psi_a + \frac{1}{2} \lambda_{mm} \psi_m^+ \psi_m^+ \psi_m \psi_m$$

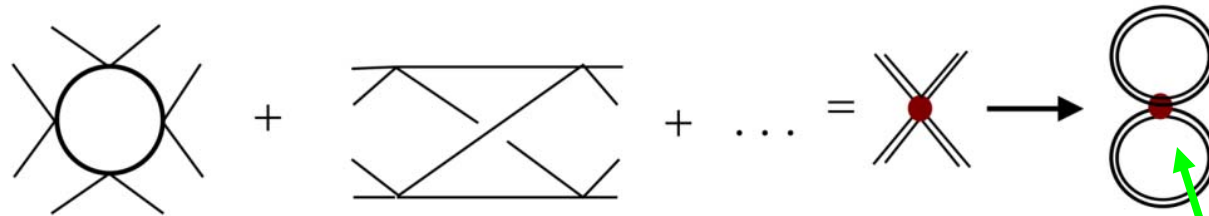
H_{am} is determined by matching.

H_a H_{am} E/V 

atom-atom vertex
(Lippmann-Schwinger eq.)



atom-dimer vertex
(Faddeev eqs.)



dimer-dimer vertex
(Yakubovsky eqs.)

Matching between the 2--, 3-- and 4--particle amplitudes computed with H_a and H_{am} . Only diagrams containing l_2 -vertices are shown.

The effective vertices thus defined (right side) can then be used to compute the ground state interaction energy in the leading order terms in an na^3 expansion, which is given by the diagrams after the arrows.

Fermi atoms

$$\lambda_{aa} = \frac{4\pi\hbar^2 a}{m},$$

$$\varepsilon_2 = -\frac{\hbar^2}{ma^2}$$

$$\lambda_{am} = \frac{3\pi\hbar^2 a_{am}}{m} = \frac{3.537\pi\hbar^2 a}{m},$$

$$a_{am} = 1.179a$$

$$\lambda_{mm} = \frac{2\pi\hbar^2 a_{mm}}{m} = \frac{1.2\pi\hbar^2 a}{m},$$

$$a_{mm} = 0.60a$$

a_{am} was first computed first by Skornyyakov and Ter-Martirosian (1957) who studied neutron-deuteron scattering.

a_{mm} was computed by Petrov (2003) and Fonseca (2003).

Consider now a dilute mixture of fermionic atoms and (bosonic) dimers at temperatures smaller than the dimer binding energy ($a > 0$ and $a \gg r_0$)

$$\frac{E}{V} = \frac{3}{5} \frac{\hbar^2 k_F^2}{2m} n_f + \frac{\pi \hbar^2 a}{m} n_f^2 + \frac{3.537 \pi \hbar^2 a}{m} n_f n_b + \frac{0.6 \pi \hbar^2 a}{m} n_b^2 + \varepsilon_2 n_b + \text{corrections}$$

$$n_f = \frac{k_F^3}{3\pi^2}, \quad \varepsilon_2 = -\frac{\hbar^2}{ma^2}$$

Even though atoms repel there is BCS pairing!

$$U_{fbf}(q, \omega) = U_{fb}^2 \frac{2n_b \varepsilon_q}{\hbar^2 \omega^2 - \varepsilon_q (\varepsilon_q + 2n_b U_{bb})}$$

$$U_{bb} = \frac{4\pi \hbar^2 a_{bb}}{m_b}, \quad \varepsilon_q = \frac{\hbar^2 q^2}{2m_b}$$

in coordinate representation at $\omega = 0$

$$U_{fbf}(r) = -\frac{U_{fb}^2}{U_{bb}} \frac{1}{4\pi \xi_b^2 r} \exp\left(-\frac{r}{\xi_b}\right)$$

$$\xi_b = \frac{\hbar}{2m_b s_s} = \frac{a_{bb}}{\sqrt{16\pi n_b a_{bb}^3}} \gg a_{bb}, \quad s_b^2 = \frac{n_b U_{bb}}{m_b}$$

One can show that pairing is typically weak in dilute systems!

Induced fermion-fermion interaction

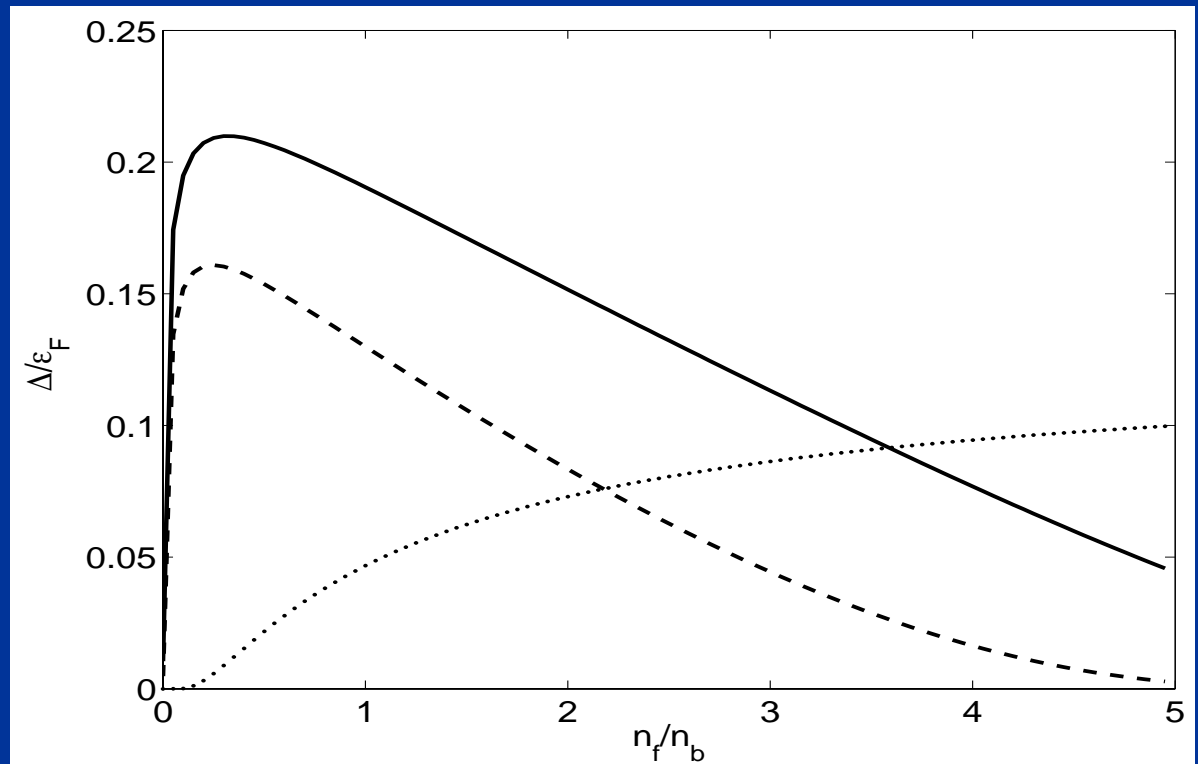
Bardeen *et al.* (1967),
Heiselberg *et al.* (2000),
Bijlsma *et al.* (2000)
Viverit (2000),
Viverit and Giorgini (2000)

← coherence/healing length and speed of sound

The atom-dimer mixture can potentially be a system where relatively strong coupling pairing can occur.

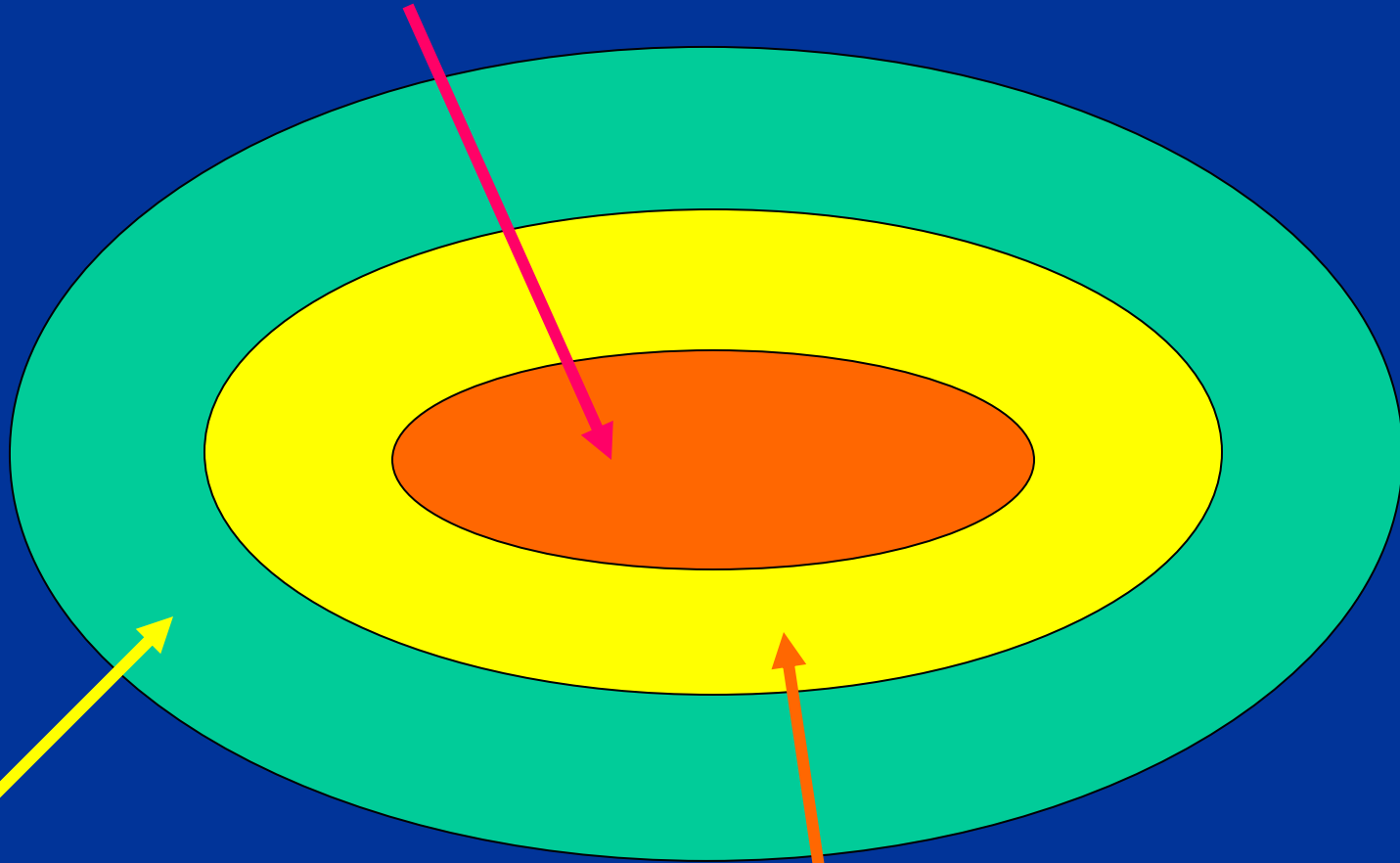
$$\Delta = \left(\frac{2}{e}\right)^{7/3} \frac{\hbar^2 k_F^2}{2m} \exp \left[\frac{2}{\pi k_F a} \left(1 - 5.21 \frac{\ln(1 + 4k_F^2 \xi_b^2)}{4k_F^2 \xi_b^2} \right)^{-1} \right]$$

$n_b a^3 = 0.064$ (solid line)
 $n_b a^3 = 0.037$ (dashed line)
 p-wave pairing (dots)



How this atomic-molecular cloud really looks like in a trap?

Core: Molecular BEC



Crust: normal Fermi fluid

Mantle: Molecular BEC + Atomic Fermi Superfluid

Everything is made of one kind of atoms only, in two different hyperfine states.

All this follows by solving the Thomas-Fermi equations:

$$\left. \begin{aligned} \frac{\hbar^2 k_F^2(\vec{r})}{2m} + \left(U_{ff} - \frac{U_{fb}^2}{U_{bb}} \right) n_f(\vec{r}) &= \mu_f - \frac{U_{fb}}{U_{bb}} \mu_b - \left(1 - \frac{2U_{fb}}{U_{bb}} \right) V(\vec{r}) \\ n_b(\vec{r}) &= \frac{\mu_b - 2V(\vec{r}) - U_{fb} n_f(\vec{r})}{U_{bb}} \end{aligned} \right\} \text{F \& B}$$

The mantle, the layer between the core and the crust.

Molecular BEC + Fermi BCS

$$\left. \frac{\hbar^2 k_F^2(\vec{r})}{2m} + U_{ff} n_f(\vec{r}) = \mu_f - V(\vec{r}) \right\} \text{F only for } V(\vec{R}_2) = \text{const} < V(\vec{r}) < V(\vec{R}_3) = \text{const}$$

The crust, the outside layer.

Normal Fermi gas

$$\left. n_b(\vec{r}) = \frac{\mu_b - 2V(\vec{r})}{U_{bb}} \right\}$$

B only for $V(\vec{r}) < V(\vec{R}_1) = \text{const}$

The core, the central region.

Molecular BEC

What happens when $|a| = 1$?

Consider Bertsch's MBX challenge (1999): "Find the ground state of infinite homogeneous neutron matter interacting with an infinite scattering length."

$$r_0 \rightarrow 0 \ll \lambda_F \ll |a| \rightarrow \infty$$

- Carlson, Morales, Pandharipande and Ravenhall, PRC 68, 025802 (2003), with Green Function Monte Carlo (GFMC)

$$\frac{E_N}{N} = \alpha_N \frac{3}{5} \varepsilon_F, \quad \alpha_N = 0.54$$

normal state

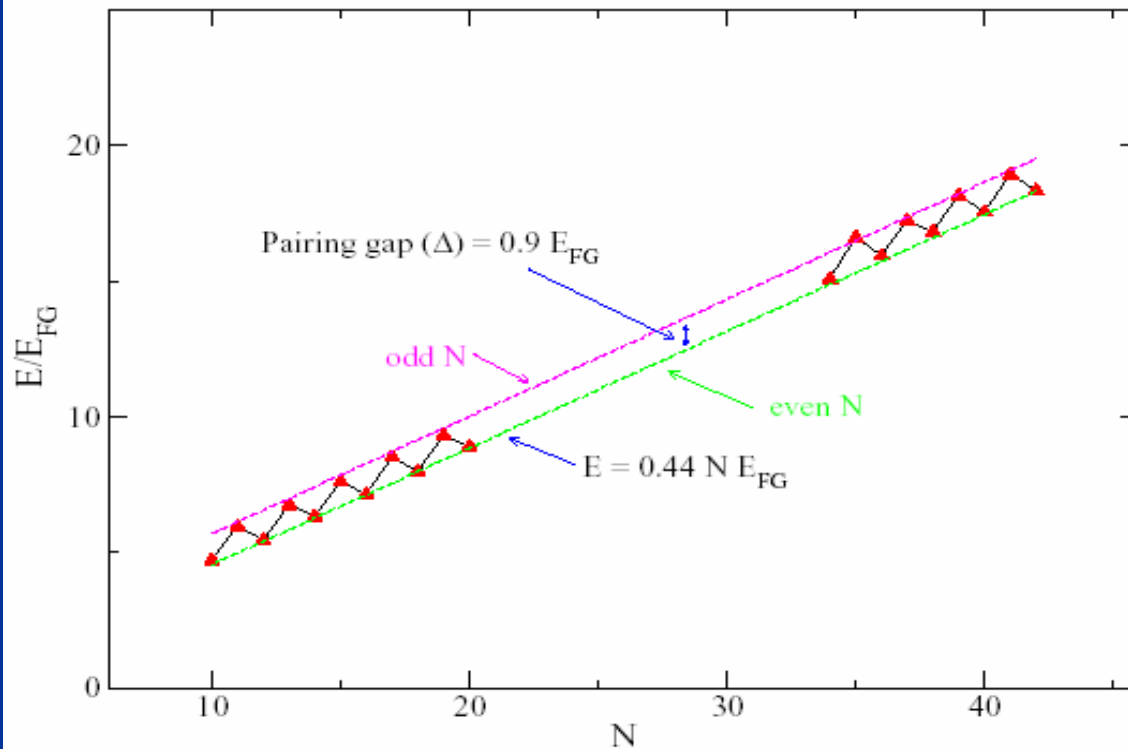
- Carlson, Chang, Pandharipande and Schmidt, PRL 91, 050401 (2003), with GFMC

$$\frac{E_S}{N} = \alpha_S \frac{3}{5} \varepsilon_F, \quad \alpha_S = 0.44$$

superfluid state

This state is half the way from BCS→BEC crossover, the pairing correlations are in the strong coupling limit and HFB invalid again.

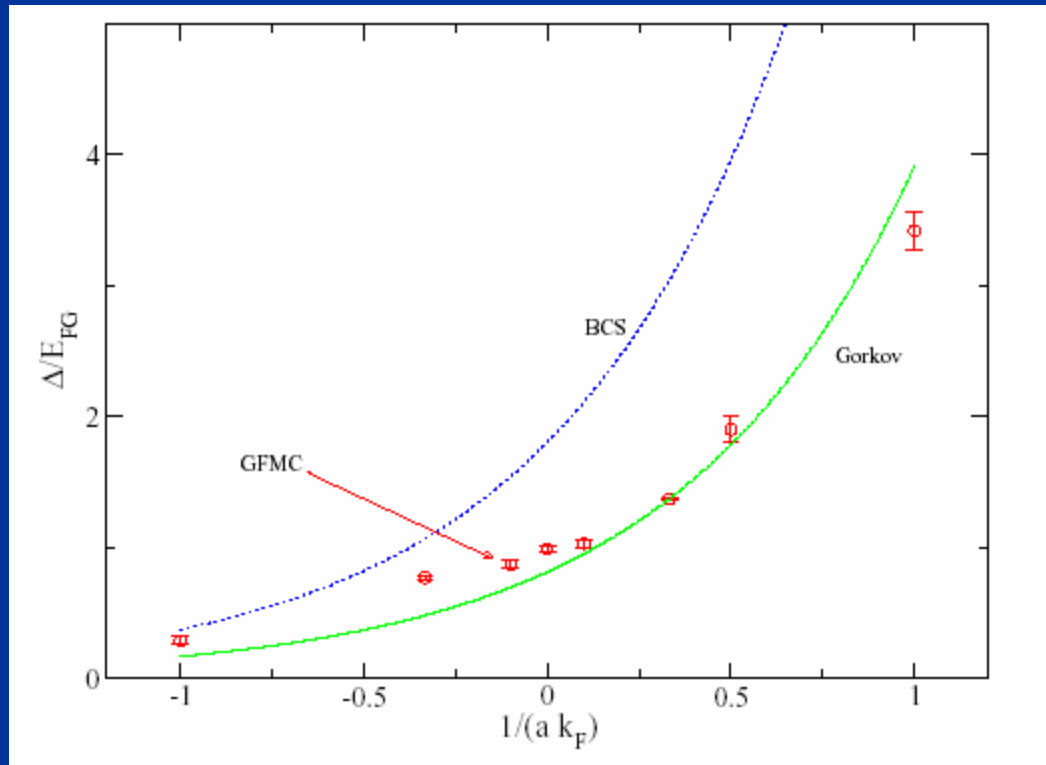
$$\Delta(2n+1) = E(2n+1) - \frac{1}{2}(E(2n) + E(2n+2))$$



$$E_{FG} = \frac{3 \hbar^2 k_F^2}{5 2m}$$

Green Function Monte Carlo with Fixed Nodes

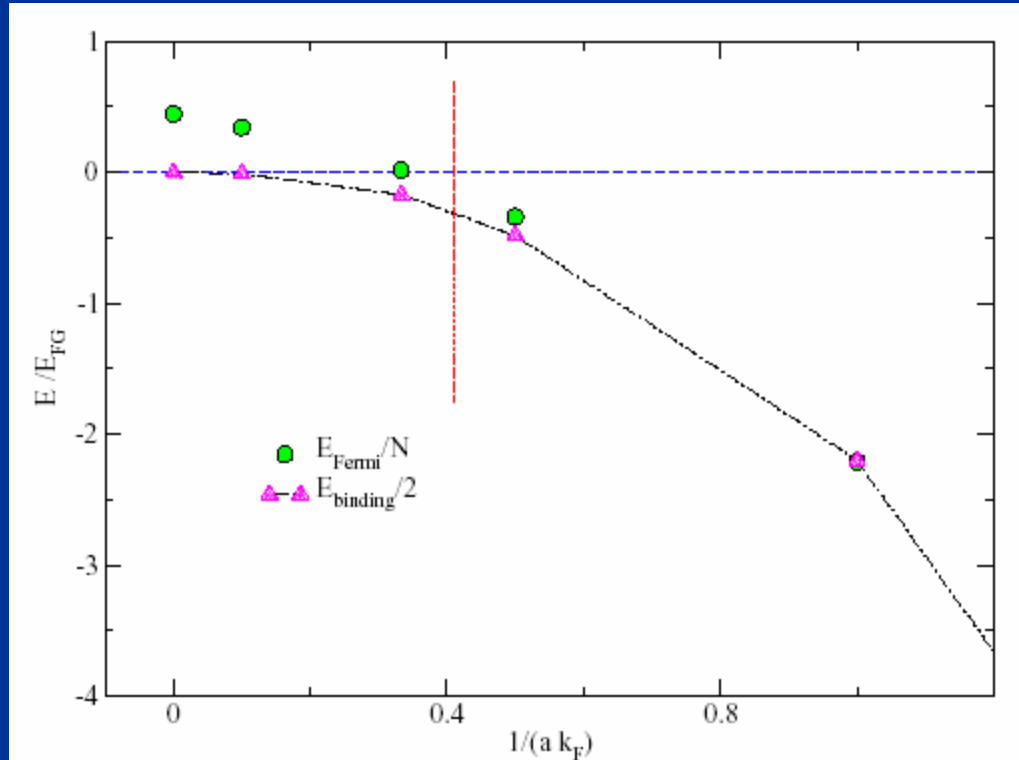
J. Carlson, S.-Y. Chang, V. Pandharipande and K. Schmidt
private communication (2003)



$$\Delta_{Gorkov} = \left(\frac{2}{e}\right)^{7/3} \frac{\hbar^2 k_F^2}{2m} \exp\left(\frac{\pi}{2k_F a}\right)$$

$$\Delta_{BCS} = \frac{8}{e^2} \frac{\hbar^2 k_F^2}{2m} \exp\left(\frac{\pi}{2k_F a}\right)$$

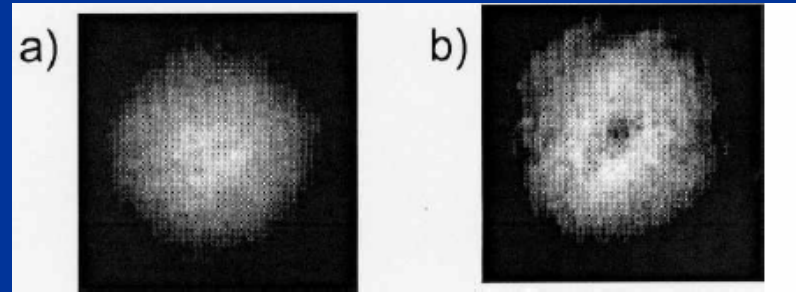
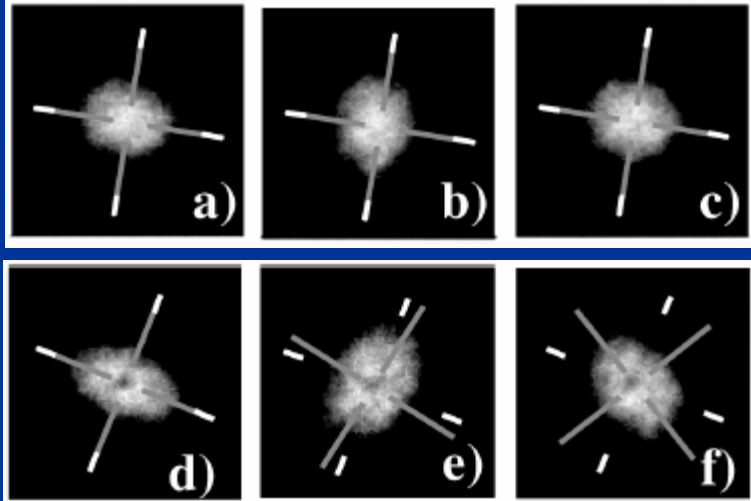
Fixed node GFMC results, J. Carlson *et al.* (2003)



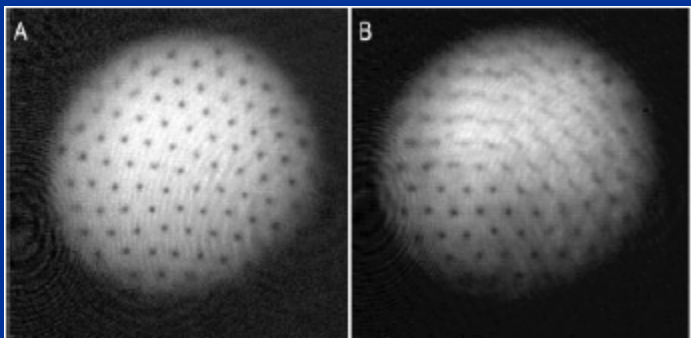
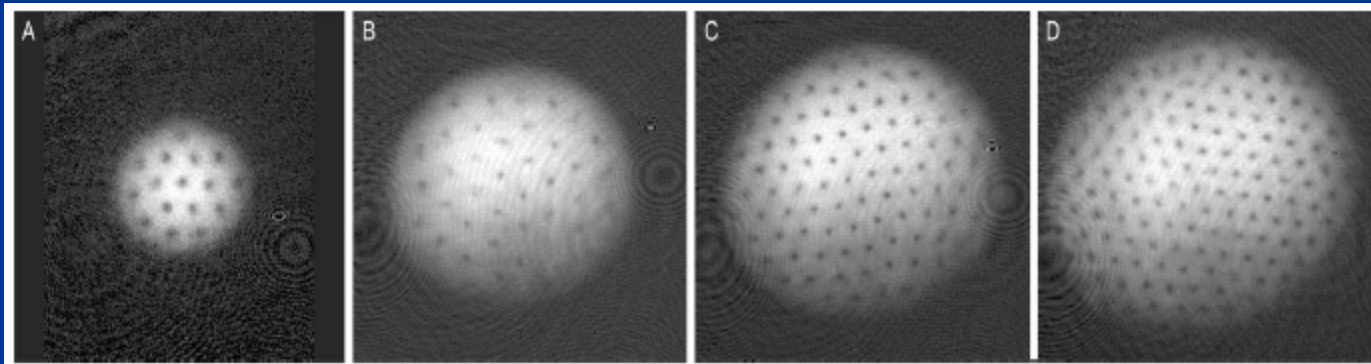
Even though two atoms can bind,
there is no binding among dimers!

Fixed node GFMC results, J. Carlson *et al.* (2003)

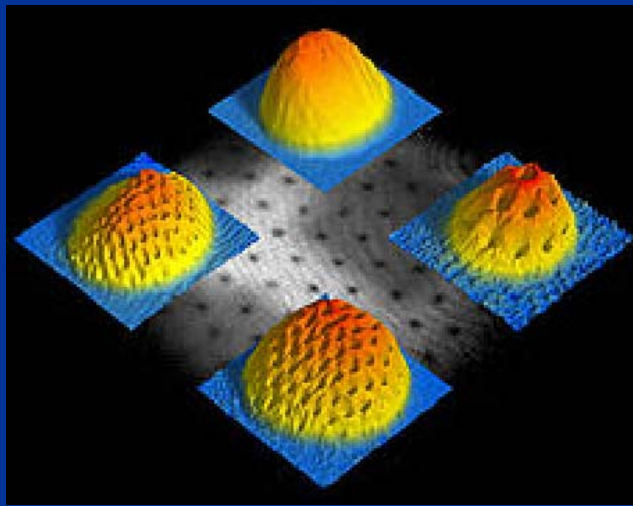
BEC Vortices



**K.W. Madison *et al*, J. Mod. Opt. 47, 2715 (2000),
F. Chevy *et al*, Phys. Rev. Lett. 85, 2223 (2000).**



J.R. Abo-Shaeer *et al*, Science, 285, 1703 (2001)



← From Ketterle's group for bosons (2001)

Why would one study vortices in neutral Fermi superfluids?

They are perhaps just about the only phenomenon in which one can have a true stable superflow!

Observation of stable/quantized vortices in Fermi systems would provide the ultimate and most spectacular proof for the existence of a Fermionic superfluid phase.

Landau criterion for superflow stability

(flow without dissipation)

Consider a superfluid flowing in a pipe with velocity v_s :

$$E_0 + \frac{Nm v_s^2}{2} < E_0 + \varepsilon_{\vec{p}} + \vec{v}_s \cdot \vec{p} + \frac{Nm v_s^2}{2} \Rightarrow v_s < \frac{\varepsilon_{\vec{p}}}{p}$$

no internal excitations

One single quasi-particle excitation with momentum p

In the case of a Fermi superfluid
this condition becomes

$$\frac{v_s}{v_F} < \frac{\Delta}{2\varepsilon_F}$$

Density Functional Theory (DFT)

Hohenberg and Kohn, 1964

$$E_{gs} = E[\rho(\vec{r})]$$

← **particle density**

Local Density Approximation (LDA)

Kohn and Sham, 1965

The energy density is typically determined in *ab initio* calculations of infinite homogeneous matter.

$$E_{gs} = \int d^3r \varepsilon[\rho(\vec{r}), \tau(\vec{r})]$$

$$\rho(\vec{r}) = \sum_{i=1}^N |\psi_i(\vec{r})|^2 \quad \tau(\vec{r}) = \sum_{i=1}^N |\vec{\nabla} \psi_i(\vec{r})|^2$$

$$-\frac{\hbar^2 \Delta}{2m} \psi_i(\vec{r}) + U(\vec{r}) \psi_i(\vec{r}) = \varepsilon_i \psi_i(\vec{r})$$

Normal Fermi systems only!

BCS wave function in infinite systems

$$|gs\rangle = \prod_{\vec{k}} (u_{\vec{k}} + v_{\vec{k}} a_{\vec{k}\uparrow}^\dagger a_{-\vec{k}\uparrow}^\dagger) |0\rangle$$

SLDA for superfluid fermi systems (AB and Y.Yu, 2003)

$$E_{gs} = \int d^3r \varepsilon(\rho(\vec{r}), \tau(\vec{r}), \nu(\vec{r}))$$

$$\rho(\vec{r}) = 2 \sum_i |v_i(\vec{r})|^2, \quad \tau(\vec{r}) = 2 \sum_i |\vec{\nabla} v_i(\vec{r})|^2$$

$$\nu(\vec{r}) = \sum_i u_i(\vec{r}) v_i^*(\vec{r}) = \langle gs | \psi_\downarrow(\vec{r}) \psi_\uparrow(\vec{r}) | gs \rangle$$

$$\begin{pmatrix} T + U(\vec{r}) - \mu & \Delta(\vec{r}) \\ \Delta^*(\vec{r}) & -(T + U(\vec{r}) - \mu) \end{pmatrix} \begin{pmatrix} u_i(\vec{r}) \\ v_i(\vec{r}) \end{pmatrix} = E_i \begin{pmatrix} u_i(\vec{r}) \\ v_i(\vec{r}) \end{pmatrix}$$

Mean-field and pairing field are both local fields!

The SLDA (renormalized) equations

$$E_{gs} = \int d^3r \{ \varepsilon_N [\rho(\vec{r}), \tau(\vec{r})] + \varepsilon_S [\rho(\vec{r}), v(\vec{r})] \}$$

$$\varepsilon_S [\rho(\vec{r}), v(\vec{r})] \stackrel{\text{def}}{=} -\Delta(\vec{r})v_c(\vec{r}) = g_{\text{eff}}(\vec{r})|v_c(\vec{r})|^2$$

$$\begin{cases} [h(\vec{r}) - \mu]u_i(\vec{r}) + \Delta(\vec{r})v_i(\vec{r}) = E_i u_i(\vec{r}) \\ \Delta^*(\vec{r})u_i(\vec{r}) - [h(\vec{r}) - \mu]v_i(\vec{r}) = E_i v_i(\vec{r}) \end{cases} \quad \begin{cases} h(\vec{r}) = -\vec{\nabla} \frac{\hbar^2}{2m(\vec{r})} \vec{\nabla} + U(\vec{r}) \\ \Delta(\vec{r}) = -g_{\text{eff}}(\vec{r})v_c(\vec{r}) \end{cases}$$

$$\frac{1}{g_{\text{eff}}(\vec{r})} = \frac{1}{g[\rho(\vec{r})]} - \frac{m(\vec{r})k_c(\vec{r})}{2\pi^2\hbar^2} \left\{ 1 - \frac{k_F(\vec{r})}{2k_c(\vec{r})} \ln \frac{k_c(\vec{r}) + k_F(\vec{r})}{k_c(\vec{r}) - k_F(\vec{r})} \right\}$$

$$\rho_c(\vec{r}) = 2 \sum_{E_i \geq 0}^{E_c} |v_i(\vec{r})|^2, \quad v_c(\vec{r}) = \sum_{E_i \geq 0}^{E_c} v_i^*(\vec{r})u_i(\vec{r})$$

$$E_c + \mu = \frac{\hbar^2 k_c^2(\vec{r})}{2m(\vec{r})} + U(\vec{r}), \quad \mu = \frac{\hbar^2 k_F^2(\vec{r})}{2m(\vec{r})} + U(\vec{r})$$

Position and momentum dependent running coupling constant

Vortex in fermion matter

$$\begin{pmatrix} \mathbf{u}_{\alpha \text{ kn}}(\vec{r}) \\ \mathbf{v}_{\alpha \text{ kn}}(\vec{r}) \end{pmatrix} = \begin{pmatrix} \mathbf{u}_{\alpha}(\rho) \exp[i(n+1/2)\phi - ikz] \\ \mathbf{v}_{\alpha}(\rho) \exp[i(n-1/2)\phi - ikz] \end{pmatrix}, \quad n - \text{half-integer}$$

$$\Delta(\vec{r}) = \Delta(\rho) \exp(i\phi), \quad \vec{r} = (\rho, \phi, z) \text{ [cylindrical coordinates]}$$

Oz - vortex symmetry axis

Ideal vortex, Onsager's quantization (one \hbar per Cooper pair)

$$\vec{V}_v(\vec{r}) = \frac{\hbar}{2m\rho^2} (y, -x, 0) \quad \Leftarrow \quad \frac{1}{2\pi} \oint_C \vec{V}_v(\vec{r}) \cdot d\vec{r} = \frac{\hbar}{2m}$$

How can one put in evidence a vortex in a Fermi superfluid?

Hard to see, since density changes are not expected, unlike the case of a Bose superfluid.

However, if the gap is not small, one can expect a noticeable density depletion along the vortex core, and the bigger the gap the bigger the depletion, due to an extremely fast vortical motion.

$$\frac{v_s}{v_F} < \frac{\Delta}{2\varepsilon_F} \propto \frac{T_c}{T_F}$$

NB T_c unknown in the strong coupling limit!

Now one can construct an LDA functional to describe this new state of Fermionic matter

$$\mathcal{E}(\mathbf{r})n(\mathbf{r}) = \frac{\hbar^2}{m} \left[\frac{m}{2m^*} \tau(\mathbf{r}) + \beta n(\mathbf{r})^{5/3} + \gamma \frac{|\nu(\mathbf{r})|^2}{n(\mathbf{r})^{1/3}} \right],$$

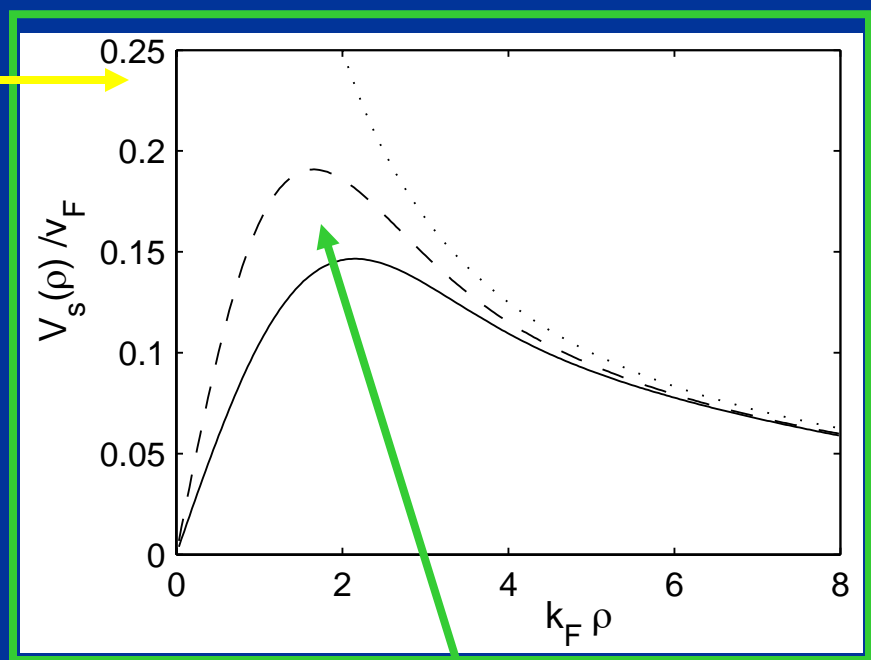
$$n(\mathbf{r}) = \sum_{\alpha} |v_{\alpha}(\mathbf{r})|^2, \quad \tau(\mathbf{r}) = \sum_{\alpha} |\nabla v_{\alpha}(\mathbf{r})|^2,$$

$$\nu(\mathbf{r}) = \sum_{\alpha} v_{\alpha}^*(\mathbf{r}) u_{\alpha}(\mathbf{r}).$$

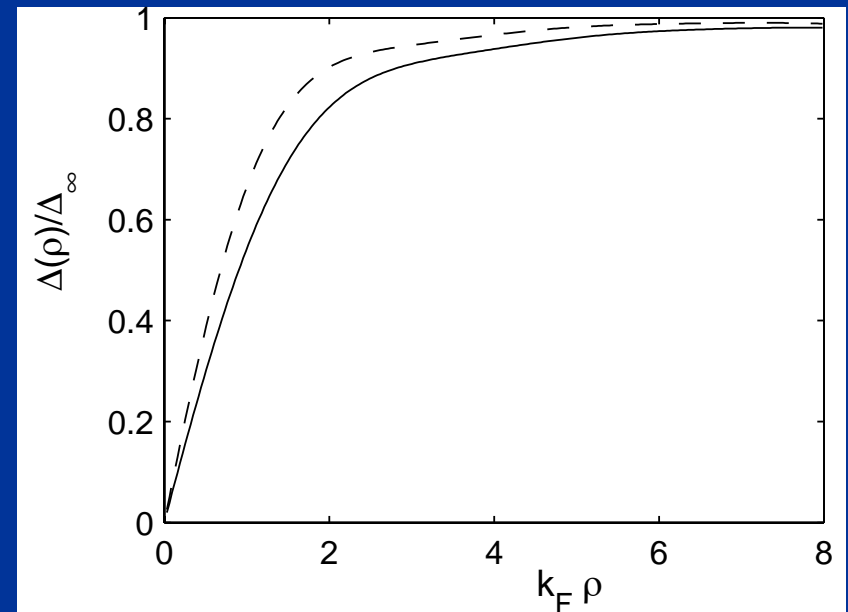
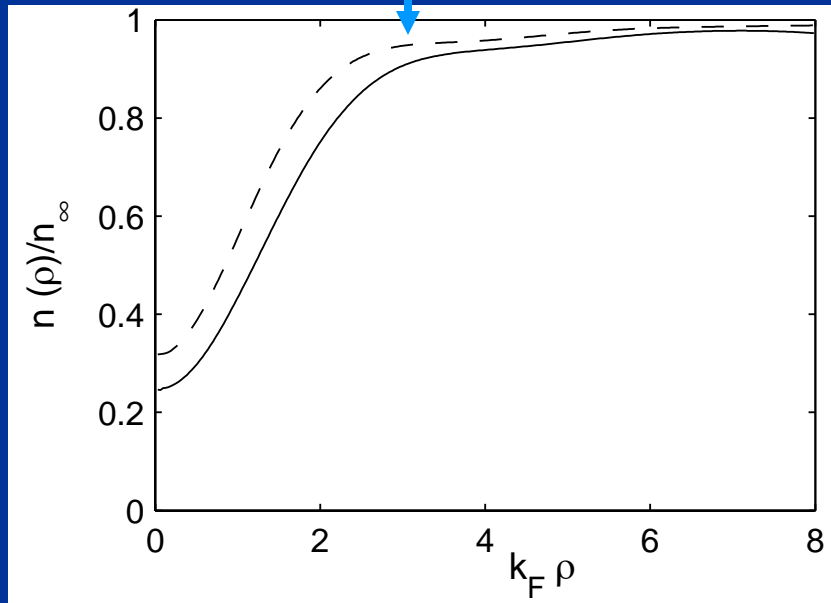
- This form is not unique, as one can have either:
b=0 (set I) or b≠0 and m*=m (set II).
- Gradient terms not determined yet (expected minor role).

Solid lines - parameter set I,
Dashed lines for parameter set II
Dots – velocity profile for ideal vortex

The depletion along the vortex core is reminiscent of the corresponding density depletion in the case of a vortex in a Bose superfluid, when the density vanishes exactly along the axis for 100% BEC.



Extremely fast quantum vortical motion!



Conclusions:

- ✓ The field of dilute atomic systems is going to be for many years to come one of the most exciting fields in physics, with lots surprises at every corner.